2018

Mechanisms by which Mechanotransduction Promotes Proliferation in Keratinocytes

Chhavi Chaudhary
South Dakota State University

MECHANISMS BY WHICH MECHANOTRANSDUCTION PROMOTES PROLIFERATION IN KERATINOCYTES

BY

CHHAVI CHAUDHARY

A thesis submitted in partial fulfillment of the requirements for the

Master in Science

Major in Biological Sciences

Specialization in Biology

South Dakota State University

2018

MECHANISMS BY WHICH MECHANOTRANSDUCTION
PROMOTES PROLIFERATION IN KERATINOCYTES
CHHAVI CHAUDHARY

This thesis is approved as a creditable and independent investigation by a candidate for a Master's in Biology degree and is acceptable for meeting the thesis requirements for this degree. Acceptance of this does not imply that the conclusions reached by the candidate are necessarily the conclusions of the major department.

Mark Messerli, Ph.D. Date
Thesis Advisor

Volker Brozek, Ph.D. Date
Head, Department of Biology and Microbiology

Kimchel Doerner Ph.D. Date
Dean, Graduate School

ACKNOWLEDGEMENTS

I would like to thank my thesis advisor Mark Messerli PhD of the Biology and Microbiology department at South Dakota State University for suggesting me the topic of this thesis and consistently supporting me to complete my MS studies and research. His guidance helped me over all of the time of research and writing of this thesis.

Besides my advisor, I would also like to acknowledge my thesis committee members Donald Augur PhD, Michael Hildreth PhD and Matthew Elliott PhD at South Dakota State University for guiding me through these two years. My committee members have been supportive and provided me with the protected academic time to pursue those goals and help me develop my own ideas.

My sincere thanks also goes to Liping Gu PhD of the Functional Genomics Core Facility at South Dakota State University for her help in offering the resources.

Finally, I must express my very profound gratitude to my parents and to my spouse Kshitij Kumar for providing me with unfailing support and continuous encouragement throughout my years of study. This accomplishment would not have been possible without them.

CONTENTS

ABBREVIATIONS

AIDS	Acquired immunodeficiency syndrome
BSA	Bovine serum albumin
$[Ca^{2+}]$	Calcium concentration
CBX	Carbenoxolone
CO_2	Carbon Dioxide
DAPI	4′,6-diamidino-2-phenylindole
DI	Deionized
DMEM	Dulbecco's Modified Eagle Medium
DMSO	Dimethyl sulfoxide
DNA	Deoxyribonucleic acid
e.g.	For example,
ECM	Extracellular matrix
EDTA	Ethylenediaminetetraacetic acid
EdU	5-ethynyl-2´-deoxyuridine
EGTA	Ethylene glycol-bis (β-aminoethyl ether)-N, N, N', N'-tetra acetic acid)
EST	Electrical stimulation therapy
FBS	Fetal Bovine Serum
Gd^{3+}	Gadolinium (III) ions
gm(s)	Gram(s)
H_2O_2	Hydrogen peroxide
H_2SO_4	Sulphuric acid
HaCaT	Human keratinocyte clonal cell line
HBSS	Hank’s balanced salt solution
hr(s)	Hour(s)
KCl	Potassium chloride
KH_2PO_4	Potassium dihydrogen phosphate
L	Liter
M	Molarity
mg	Milligram
$MgCl_2$-$6H_2O$	Magnesium Chloride Hexahydrate
$MgSO_4$-$7H_2O$	Magnesium Sulfate Heptahydrate
min(s)	Minute (s)
MK886	3-[3-butylsulfanyl-1-[(4-chlorophenyl) methyl]-5-propan-2-yl -indol-2-yl]-2,2 -dimethyl-propanoic acid
ml	Milliliter
ML204	4-Methyl-2-(1-piperidinyl)-quinoline
mM	Millimolar
MSCs	Mechanosensitive channels

Na_2HPO_4	Disodium phosphate
NaCl	Sodium chloride
$NaHCO_3$	Sodium bicarbonate
nL	Nanoliter
NPWT	Negative pressure wound therapy
PBS	Phosphate Buffer Saline
PBST	Phosphate-Buffered Saline/Triton X-100
PDMS	Polydimethylsiloxane
Pen-strep	Penicillin-Streptomycin
pS	Pico Siemen
RN1734	2,4-Dichloro-N-isopropyl-N-(2-isopropylaminoethyl) benzene-sulfonamide
ROS	Reactive oxygen species
rpm	Revolutions per minute
sec(s)	Second or seconds
S-phase	Synthesis phase
TRITC	Tetramethylrhodamine
v/v	Volume concentration or percent volume
w/v	Mass concentration or mass per unit volume
w/w	Percent mass or mass fraction
µL	Microliters
µM	Micromolar

SYMBOLS

$	Dollar (currency)
%	Percentage
*	Asterisk for statistical significance
×	Multiplication sign
<	Less than
≥	Greater than or equal to
:	Ratio
&	And
~	Approximately
°C	Degree Celsius
10X	Magnification of ten times life size
20X	Magnification of twenty times life size
2D	Two-dimensional space
3D	Three-dimensional space

LIST OF FIGURES

LIST OF TABLES

ABSTRACT

MECHANISMS BY WHICH MECHANOTRANSDUCTION

PROMOTES PROLIFERATION IN KERATINOCYTES

CHHAVI CHAUDHARY

2018

Chronic wounds are wounds that do not heal within 30 days and often they can last over a year. Interference in any of the wound healing stages may hinder the process. Some of the local and systemic factors such as infection, old age, diabetes, AIDS, and the regular application of corticoids may also have negative effects on the healing process. Cell proliferation is an important phase in epidermal wound healing in which surviving epithelial cells replicate independently into daughter cells through mitosis and maintain a balance between cell growth and cell loss during the cell cycle. Physical and chemical stimuli play important roles in regulating cell proliferation through activating intracellular signal transduction pathways. A physical stimulus which enhances skin cell proliferation relies on mechanical stretch. However, the mechanism(s) by which cells sense and respond to mechanical stimulation remain(s) unknown.

Most research regarding sensing of mechanical stimuli emphasizes the role of cellular membrane proteins including channels, integrins, and receptors for growth factors. Channels could be selective or non-selective, or mechanosensitive for inorganic ions or small molecules, with high permeability to ions such as sodium, potassium, calcium, and magnesium. Mechanosensitive channels (MSCs) are present in many cell types including epidermal keratinocytes. MSCs play a crucial role as a mechanosensors which convert mechanical stimuli into electrical or chemical signals. MSCs may affect

cells through the movement of specific ions, such as calcium, across the plasma membrane. Cytosolic calcium in the form of steady or transient changes is required for cell cycle progression, cell proliferation and cell division. In other words, Ca^{2+} influx is required for mechanosensitive cell proliferation in human keratinocytes. In this study, we monitored the proliferation rate of stretched cells and observed that mechanical stretching induces a higher percentage of keratinocytes into S-phase. Proliferation was reduced or inhibited in the absence of extracellular Ca^{2+} or when Ca^{2+} influx was blocked, respectively. Many pharmacological inhibitors of MSCs were screened to evaluate their effect on cell proliferation and the results demonstrate that blockage of the mechanosensitive ATP channel, pannexin, significantly inhibited proliferation. Identification of a pathway that promotes proliferation of keratinocytes provides us with a target for a chemical treatment that speeds proliferation and promotes wound healing.

INTRODUCTION

Skin is the largest organ of the body and it covers most of the external surface of the body. It consists of the outermost epidermis and the underlying dermis. Some have listed the hypodermis, a layer beneath the dermis as a third layer of skin (1). Skin is supported by several underlying structures including fascia (connective tissue), muscle, tendons, ligaments, and arterial and venous blood vessels (2). It is a defensive and sensory barrier between the external environment and the internal organs which protects against water loss, damaging chemicals, micro-organisms, mechanical stress, and radiation. Skin has sensory functions related to touch, pressure, temperature, and pain, and alerts the body to potential tissue damage (3-7).

The epidermis is the outermost layer of the skin comprised of nearly 95% keratinocytes, but also includes melanocytes, Langerhans cells, and Merkel cells (8). It works as a waterproof barrier which repels fluids but retains water in the body. Its thickness varies from 0.07 mm to 0.12 mm, except on the palms and soles, where it varies from 0.8 mm to 1.4 mm (9). The epidermis does not contain any blood vessels, however, even the deepest layer of epidermis obtains some O_2 which diffuses in from the external atmosphere.

Cells of the epidermis replicate through mitotic division at the deepest layer and the cells move superficially to the outermost layer. The cells change shape and composition during their movement through the epidermis. The outermost layer of the epidermis is approximately 25 times thicker than the basement membrane layer (10). This process takes place within weeks. Below is a detailed description of the five different layers of epidermis from deep to superficial.

1. The basal layer of epidermis is known as the stratum basale and contains keratinocytes, melanocytes, and Merkel cells. The keratinocytes, from the lowest layer of the epidermis, are continually moving to the outermost surface by the production of new cells beneath them. Keratinocytes fill with keratin as they are pushed to the surface of the epidermis and this process is known as keratinization.

2. The stratum spinosum is the second layer superficial to the stratum basale where keratinocytes begin to develop cell-cell junctions and begin producing lamellar bodies, secretory granules filled with lipids, hydrolytic enzymes, and many other proteins.

3. In the next layer, the stratum granulosum, keratinocytes lose their nuclei and the cytoplasm is more packed with lamellar bodies.

4. The stratum corneum is the outermost layer which is made of the mature or dead keratinocyte epithelium. Keratin protein in the stratum corneum layer moves superficially and these cells are sloughed off from the surface constantly. The stratum corneum has an acidic pH, called the acid mantle, which protects the body from some bacteria and fungi. Most of the barrier function of the epidermis is contained in this outer most layer.

5. The palms of the hands and the soles of the feet contain a 5^{th} epidermal layer, called the stratum lucidum, a clear inner layer of the stratum corneum. This layer is made of dead and flattened cells.

Epidermal Wounds

Epidermal wounds occur when skin is cut, punctured, or damaged through some other form of injury such as ischemic injury which occurs during prolonged blood restriction. Injuries can damage the epidermal and dermal cells, nerves, blood vessels and other underlying tissues, and even organs. Based on the cause of damage, site, depth, and duration to heal, wounds can vary from simple to life threatening. According to the healing time, wounds can be classified as acute or chronic and a descriptive comparison between these two groups of wounds is listed in Table 1 below (11, 12).

Table 1. Acute vs. chronic wounds.

Parameter	Acute Wound	Chronic wound
Duration	wounds that heals within expected period. e.g. weeks to months	wounds that do not heal within anticipated time. e.g. one month to three months
Symptoms	pain, swelling or bleeding, foul smelling pus or drainage	signs are noticeable but unknown or unclear such as erythema, edema, heat, or severe inflammation
Examples	surgical wounds, bites, burns, abrasions trauma	venous stasis ulcer, diabetic foot ulcer, bedsores, pressure ulcer and arterial ulcer
Wound Assessment	chemical treatment, minimal mediation, surgical debridement, antimicrobial therapy	no chemical treatment, wound dressing, negative pressure therapy, electrical stimulation

Wound healing requires many important factors to work in a coordinated manner. Non-healing wounds are wounds which fail to heal through the normal process or in a timely manner (13). Chronic wounds generally last more than 30 days but can last for over a year. Multiple factors affect the wound healing process and they can be divided into two classes depending on their source. First, local factors affect the patient from the external environment including dehydration of the wound, microbial load, level of

maceration, necrosis, pressure, trauma, and edema. On the other hand, systemic factors directly affect the performance of bodily functions through the patient's own physiology or condition such as age, gender, diabetes, obesity, hypothyroidism, immunosuppression, radiation therapy or chemotherapy, macronutrients or micronutrients and smoking (14-18).

Chronic wounds are the result of vascular ulcers (e.g., venous and arterial ulcers), diabetic ulcers, and pressure ulcers (19). Some common features shared by each of these wounds include prolonged or excessive inflammation (20), persistent infections (21), formation of drug-resistant microbial biofilms (22), and the inability of dermal and/or epidermal cells to respond to reparative stimuli (23-25). Altogether, these pathophysiological phenomena result in the failure of these wounds to heal. The underlying pathologies, however, differ among various types of chronic wounds.

Chronic wounds have been a major challenge for both patients and the healthcare system throughout the world. It has been estimated that the annual chronic wound costs exceed $15 billion with the chronic wounds affecting approximately 2.4–4.5 million patients, in the United States alone (26-28). It has been reported that the cost to treat chronic wounds in the USA is 2-3% of the healthcare budget in other developed countries and it represents approximately 2% of total European Union financial resources, Table 2 (27, 29, 30).

Table 2. Summary of the impacts of chronic wounds (30)

Type	No. of affected patients	Cost of treatment	Total annual cost
Venous ulcers	400,000–600,000	$5,000–$10,000	$1.9 - $2.5 billion (31)
Arterial ulcers	100,000 (32)	$9,000–$16,000	
Diabetic ulcers	2 million	$6,000/patient	$150 million (33)
Pressure ulcers	1.3 - 3 million	Up to $70,000 (34)	$3.5 - $7.0 billion (34)

The chronic wounds listed above are more commonly found in elderly patients and the elderly population in the USA continues to increase. The number of citizens 65 years or older is expected to nearly double (from 35 million to 53 million people) by 2030 (35) and the estimated risk of developing diabetes for children born in 2000 is as high as 35% (36). The anticipated risks of diabetes and age-associated nonhealing chronic wounds continue to increase dramatically, and the estimated chance of diabetes and age-associated chronic wounds will increase in the future and throughout the world.

The medical treatment for chronic wounds often uses advanced treatments such as growth factors, extracellular matrices (ECMs), engineered skin, Electrical stimulation therapy (EST) and negative pressure wound therapy (NPWT) (37). The latter two treatments have been used to speed the healing of chronic wounds. Both appear to make use of mechanotransduction pathways to promote healing.

Epidermal Wound Healing

Epidermal wound healing is a crucial and complicated process to repair the strength and missing portions of the organ to regain structure and function. Four-stages

are involved in epidermal repair and reconstruction including hemostasis, inflammation, proliferation, and maturation.

The first phase of healing is known as hemostasis, in which bleeding is stopped. Platelets bind with collagen outside of the bloodstream to promote platelet plug formation. The release of other chemical messages promotes activation of clotting factors, including thrombin, to form the fibrin mesh to prevent further loss of blood.

Preparation of the wound bed for the growth of new tissue is part of the defensive or inflammatory phase of wound healing. This is done by the process of phagocytosis in which white blood cells invade the injured site and engulf bacteria and remove foreign material or debris from the wound within 2 days. Release of growth factors including platelet derived growth factor (PDGF) and vascular endothelial growth factor (VEGF) are also released and lead to the beginning of the proliferative phase.

The formation of new blood vessels and filling of the wound bed through granulation occurs during the very early stage of the proliferative phase. Then, construction of the wound margin takes place. Migration of epithelial cells from the edges of the wound toward the center of the wound occurs. The process continues until the epithelial cells cover the wound completely.

The last phase of wound healing is known as maturation or the remodeling phase. New tissue is remodeled and matures to attempt to recover the original strength and flexibility. Unused cells will undergo apoptosis or programmed cell death.

Most cells are sensitive to different forms of mechanical stimuli. Different physical forces are important for the regulation of cell physiology and pathogenesis of skin. Mechanotransduction is the process by which cells sense mechanical forces from

the surrounding environment and convert these physical forces into appropriate biochemical signals. Forces are required to maintain cell shape and function, during proliferation, migration, and apoptosis. The mechanosensitive nature of tissues is well known and is used to help drive development of better medical devices, novel drugs, and therapies for treating diseases, and novel tissue scaffolds for tissue repair and reconstruction (38-42).

There are many signaling pathways by which cells respond to mechanical stress. It is now apparent that there are also multiple types of mechanoreceptors, ranging from stretch-activated channels in the plasma membrane, to cytoplasmic proteins, and the nucleus itself undergoes changes in response to force. However, the exact mechanisms by which a cell senses and reacts to mechanical signals are not entirely unknown. Over the past few decades, the importance of mechanical signals in tissue development, homeostasis and repair have been recognized, and the underlying mechanisms are being actively identified.

Cells are subjected to various combinations of mechanical stimuli in their physiological environment. Hence, it is difficult to predict which stimulus is responsible for which change within the cell. To understand the nature of physical forces, 3 different forces will be discussed, including compression, tension, and shear (43).

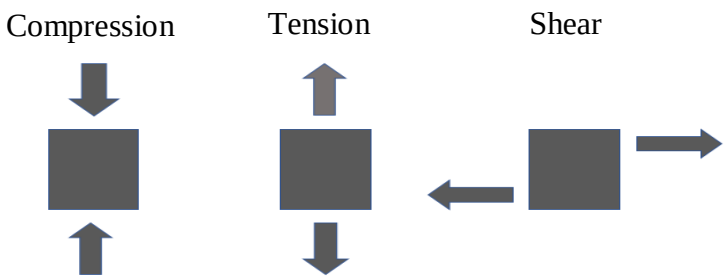

Figure 1. Different types of mechanical forces.

Compression

Compression is known as a pushing force and leads to a decrease in the length of the object along a specified axis.

Tension

Tension is a pulling force that tends to stretch the material in opposite directions. An increase in blood pressure increases tension on the endothelial cells while a rapid increase in weight gain places an increase in tension on the epidermis. Stretching of epidermal keratinocytes promotes proliferation to reduce the stretching force (44-47).

A common way to apply tension to cells is to seed them on a stretchable surface. After cells have adhered to the stretchable surface, the substrate is stretched in opposite directions from two ends and the adherent cells become stretched as well.

Shear

Shear is a force which tends to slide one face of an object over an adjacent face. It can bend or twist the object. The endothelial cells lining blood vessels are subject to shear stresses produced by blood flow (48).

The process of cellular mechanotransduction is divide into three stages:

(i) Mechanoreception: Detection of the stimulus and transmission of the signal from outside the cell to the inside.

(ii) Intracellular signal transduction: Transduction of mechanical stimulus into biological signals in the cell where a series of signaling response can be generated. The intracellular signal is transmitted by second messengers, and a network of intracellular signaling proteins.

(iii) Target activation: Activation of proteins that causes changes in cell structure and function in response to stretch.

Mechanoreceptors respond to extracellular physical signals and transmit these extracellular stimuli from the outside of the cell to the inside. Mechanoreceptors are commonly present in the cell membrane including (i) integrins, (ii) mechanosensitive or stretch-activated channels, and (iii) other cell-surface receptor proteins. This thesis will emphasize plasma membrane, mechanosensitive channels.

Mechanosensitive Channels

Mechanosensitive or stretch-activated channels (49-54) are proteins that span the plasma membrane, connecting the cytosol to the cell exterior. The permeability of ion channels is highly controlled. However, while some channels are most permeable to only one ion e.g. Na^+, K^+, Ca^{2+}, and Cl^-, some are non-selective and allow multiple cations or anions to pass through, while others allow passage of small organic molecules. In the resting state many mechanosensitive channels are usually closed. Introduction of a mechanical stimulus shifts the channels to an open state and ions or molecules move down their electrochemical gradient. Mechanosensitive ion channels are the sensors for several systems including the senses of touch, hearing, and balance, as well as participating in cardiovascular regulation and osmotic homeostasis (55-57).

Based on the permeability of ions, mechanosensitive ion channels can be divided into different groups. Cation-selective MSCs show a selective permeability for positive ions such as Na^+, K^+ and Ca^{2+}. They exhibit a small single channel conductance range of 25-35 pS (54). These cation-selective MSCs are blocked by the trivalent gadolinium ion. Anion selective MSCs are permeable for negative ions and generally contain a large

conductance (> 300pS). Non selective ion channels are found in the Archaea and prokaryotes, and rarely in Eukarya (58).

Examples of Mechanosensitive channels in Eukaryotes -

1. ENaC/DEG superfamily (59)
2. TRP superfamily: There are seven subfamilies within the TRP superfamily: TRPC (canonical), TRPV (vanilloid), TRPM (melastatin), TRPP (polycystin), TRPML(mucolipin), TRPA (ankyrin), and TRPN (NOMPC-like) (59)
3. Piezo1 and Piezo2 (60)
4. Pannexin (61)

Cells are mechanically stimulated through several major interrelated pathways which include integrin–matrix interactions, cytoskeletal strain, and membrane stress. Two mechanisms are supposed to be responsible for the opening of mechanically gated ion channels. First, the conformation of ion channels is modified in response to applied forces that affect the membrane-embedded proteins. This is known as lipid bilayer tension or the stretch method (62, 63). Second, stretch activated channels have an ability to be deformed by the actin cytoskeleton or extracellular matrix which is attached to the stretch-activated channel and they directly regulate the opening of ion channels (55, 64). This process is known as the spring-like tether model. In addition, mechanosensitive channels control calcium-dependent pathways that further regulate intracellular signaling and cytoskeletal remodeling (65-67).

Mechanical Forces Promotes Cell Proliferation

Mechanical forces regulate various phases of the cell cycle which include the onset of mitosis. Researchers found that the tension and mechanical energy of a tissue

could anticipate the regulation and duration of the phase G1–S transition and mitotic rounding. Cells that experience the higher intercellular tension exhibit a higher probability to transition from G1 to S, as well as a shorter G1 and shorter S–G2–M phases. It is also found that tension increases during the cell cycle but decreases 3 hours before mitosis to facilitate the process of mitosis. In addition, neighboring cells collaborate in this process before and during division (44-47).

The research in this thesis will be directed toward understanding the Ca^{2+} influx pathway that is used by keratinocytes to promote proliferation. Cells cultured on a flexible silicone membrane, will be stretched and multiple pharmacological blockers will be screened to help identify this pathway. We hypothesize that the pathway that is used to promote keratinocyte proliferation, could be stimulated chemically to help promote cellular proliferation and speed wound closure.

MATERIALS AND METHODS

Cell Culture

Clonal human epidermal keratinocytes, HaCaT, were maintained in Dulbecco's Modified Eagle Medium (DMEM, Gibco, Fisher Scientific) containing 10% Fetal Bovine Serum (Gibco, Fisher Scientific), 1% of 10,000 index units of penicillin-streptomycin solution. Cells were cultured in a 5% CO_2, 37° C, humidified incubator. For experimentation, cells were seeded on polydimethylsiloxane (PDMS) chambers in normal DMEM medium (Appendix A) for 24 hrs. Optimum cell density for seeding the cells on the PDMS chambers was ~$1x10^5$ cells/ml). Cell density was determined prior to seeding the PDMS chambers by counting cells with a hemocytometer.

Preparation of Cell Suspension for Splitting or Transferring Cells

Removing cells from the bottom of the tissue culture flask prior to splitting the culture to a different flask or prior to seeding cells in the PDMS chambers required gentle removal of those cells using a trypsin-EDTA solution. EDTA chelates divalent ions and loosens cells from the bottom of the dish while trypsin, a protease, cuts protein connections between the cells and the bottom of the flask. The protocol below is used to prepare the cell suspension:

1. Gradually remove the DMEM from flask with adherent cells.
2. Rinse cells with brief treatment, < 20 s, of 2 ml of 0.25% trypsin-EDTA.
3. Add 2 ml of 0.25% trypsin-EDTA and keep in incubator for 3-5 mins to dissociate adherent cells from the bottom of the flask.
4. Add 10 ml of DMEM to halt trypsin activity.

5. Gently transfer the cells into a 15 mL conical tube and centrifuge the cells at 800-1000 rpm, 5 mins, to pellet the cells and remove dilute trypsin-EDTA.
6. Remove the dilute trypsin-EDTA and DMEM from the conical tube.
7. Submerge the cell pellet with 1mL of DMEM and gently resuspend the cells.

Counting Cells with the Hemocytometer

Cell numbers are determined by using a hemocytometer. Hemocytometers are essentially a grid, etched into a glass slide with a coverslip placed a known distance from the bottom of the slide (Figure 2). Therefore, a 2D cell count can be calculated to determine a 3D cell density.

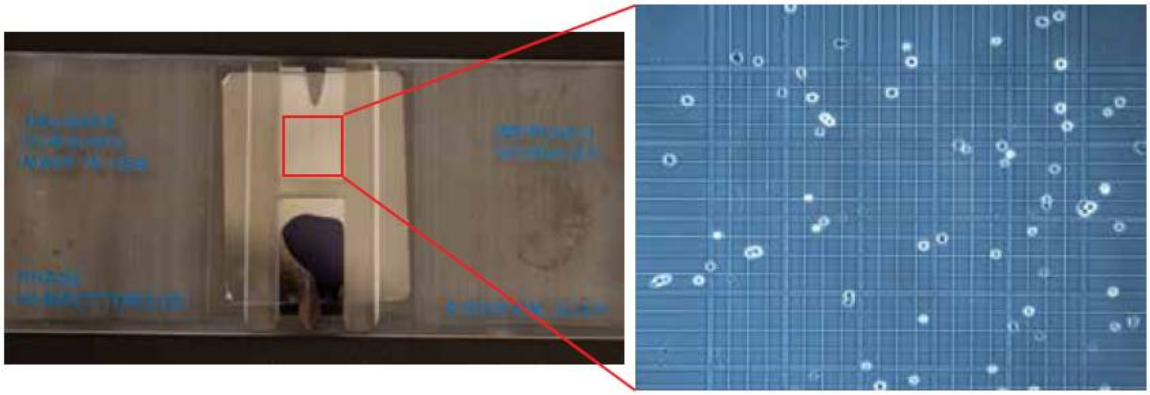

Figure 2. Example of a hemocytometer.
("Hemocytometer" by Matt Janicki. CC BY 2.0. https://creativecommons.org/licenses/by/2.0/#)

The following protocol is used to prepare and count cells on a hemocytometer.

1. Hemocytometer and glass coverslip should be cleaned with ethanol before use.
2. Place 10 µl of 5x diluted cell suspension on the hemocytometer grid and cover with coverslip.
3. Using an upright microscope, focus on the grid lines of the small, internal squares with a 10x microscope objective.
4. Count the live cells within 16 small squares (4 by 4 squares) with volume of 4 nL.

5. Move the hemocytometer and count 3 addition 4 by 4 boxes, along the corners of the hemocytometer grid.
6. Take the average of cells from all of the regions.
7. Divide by 4 x 10^{-6} mL to obtain cells/mL and multiply by 5 to correct for the dilution.
8. The final cell count is the number of viable cells per ml in the original cell suspension.

Preparation of Silicone Chambers

The SYLGARD ® 184, silicone elastomer kit (Dow Corning) is used to prepare the PDMS chambers. PDMS chambers (68) were prepared by mixing, uncured polymer and curing reagent in [10: 0.86 (w/w)] for 10-15 s. The mixture was degassed at room temperature and cured at 37°C overnight in a plastic mold (Figure 3). The mold includes removable aluminum pylons in order to enable attachment to a stretching rack. Additionally, small rectangular pieces of polycarbonate were inserted in the bottom of the mold prior to PDMS in order to fabricate a well in the PDMS chamber (Figure 3). After curing, chambers were treated to enable cell adhesion to the hydrophobic silicone.

Surface Modification of PDMS Chambers

The hydrophobic silicone surface was made more hydrophilic through oxidation with piranha solution, a mixture of concentrated H_2SO_4 and 30% H_2O_2 in a 3:1 ratio (69). This mixture is exothermic and was allowed to cool to room temperature before applying on chambers. Over oxidation of the chambers caused an opaque surface and even rippling at higher oxidation which made imaging of cells difficult. Also curing times varied with

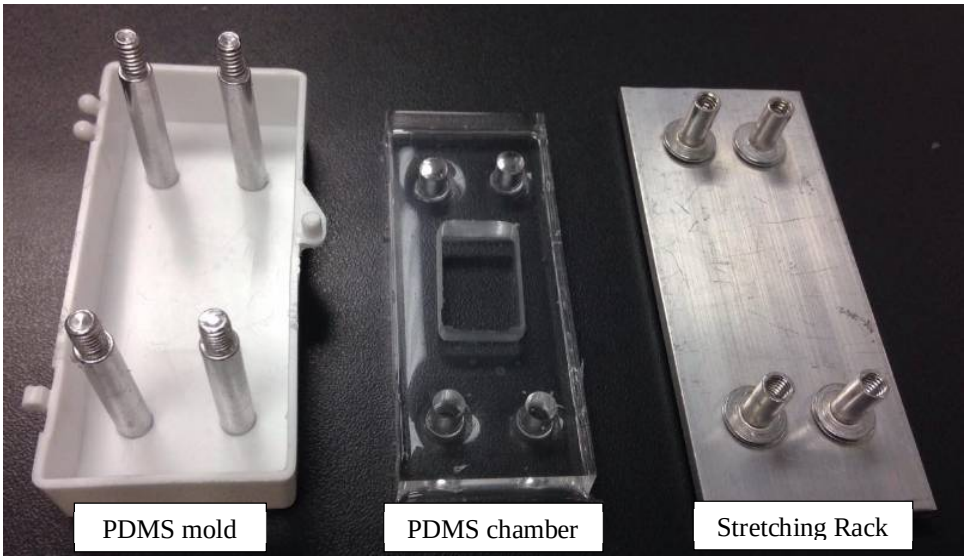

Figure 3. PDMS chamber mold, finished PDMS chamber and stretching rack.

The pylons of the stretching rack are 10% further apart than the pylons in the mold so that when the chamber is mounted on the rack, the PDMS will be stretched by 10% different batches of the purchased starting materials. Therefore, a test oxidation was performed for each batch. A successful test was determined by the absence of opaqueness after oxidation when dried. As a result, oxidation with piranha solution varied from 30s to 5 mins at room temperature. After oxidation, chambers were rinsed with DI water.

To ensure removal of oxidation products and piranha solution from the chambers they were soaked in DI water for 10 mins in repetition. PDMS is porous and repetition of this process enhanced cellular adhesion on the chambers.

Silicone Chamber Sterilization and Coating with Collagen

Cell adhesion was enhanced through collagen coatings. Chambers were sterilized with 70% ethanol and allowed to dry for 30 mins in a sterile, laminar flow hood. Collagen (Advanced Biomaterial Pure Collagen type I) was diluted in sterile filtered, DI water, 1:30

(v/v). The mixture was spread on the chambers in order to allow the collagen protein to bind on the chambers at room temperature for 2-3 hours (68). Fluid was removed and the chambers were allowed to air dry in the sterile hood for 30-60 mins. Collagen coated chambers were used immediately after drying or stored at 2-8°C until use. Before introducing cells, collagen coated chambers were gently rinsed with PBS or culture medium to remove any nonadherent collagen and to ensure neutral pH during cell adhesion. A step by step protocol for chamber preparation is provided in Appendix B.

Stretch-Induced Cell Proliferation Assay

HaCaT cells were plated on sterilized and collagen-coated, PDMS chambers with similar cell density so that cells could grow on the chamber surface for 48 hours. Cells were initially plated in DMEM to inactivate residual trypsin and enhance adhesion. After 4 hrs incubation, unattached cells were removed by washing with fresh Hank's media (70) and adherent cells were incubated for 24 hours at 37°C before stretching (71). During experiments, cells were stretched on aluminum stretching racks (Figure 3) and fresh Hank's media was added to the chambers. Overnight cultures of cells were exposed to unstretched and stretched conditions in attempts to identify the mechanosensitive signaling pathway which promotes cell proliferation. Three hours before the end of the 24 hour stretching period (68), the EdU (5-ethynyl-2'-deoxyuridine) reagent was added on the chambers. EdU is a nucleoside, a thymidine analog which has been chemically modified for easy fluorescent tagging. Cells in the proliferation phase of the cell cycle incorporate EdU into their nuclei during DNA replication. The EdU reagent enables identification of the relative numbers of cells within the S-phase of the cell cycle which precedes mitosis.

Preparation of Hank's Balanced Salt Solution (HBSS)

Serum free, HBSS was used during experimentation as HaCaT cells show a 2.5-fold increase in proliferation during 10% stretch in HBSS (70, 71). HBSS was made by adding each of the components from Table 3. Media was filter sterilized and stored at 4°C in the refrigerator.

Table 3. Composition of HBSS (1L).

Component	Mass	Molarity
NaCl (mw: 58.4 g/mol)	8 g	0.14 M
KCl (mw: 74.6 g/mol)	400 mg	0.005 M
$CaCl_2$ (mw: 111.0 g/mol)	140 mg	0.001 M
$MgSO_4$-$7H_2O$ (mw: 246. 5 g/mol)	100 mg	0.0004 M
$MgCl_2$-$6H_2O$ (mw: 203.3 g/mol)	100 mg	0.0005 M
Na_2HPO_4 (mw: 178.0 g/mol)	60 mg	0.0003 M
KH_2PO_4 (mw: 136.1 g/mol)	60 mg	0.0004 M
Glucose (mw: 180.2 g/mol)	1 g	0.006 M
$NaHCO_3$ (mw: 84.0 g/mol)	350 mg	0.004 M

Pharmacological Blockers

Pharmacological blockers of mechanosensitive channels were added in the culture media in attempts to block stretch-induced proliferation. Blockers were made as stock solutions in aqueous media or dimethyl sulfoxide (DMSO) for the more hydrophobic agents (Appendix A). For example, a 10 mM stock solution of amiloride was dissolved in DMSO and diluted in HBSS prior to experimentation to obtain a final working concentration of 10 μM. Other compounds were diluted to final working concentrations listed in Table 4.

Table 4. List of pharmacological blockers of mechanosensitive channels.

Blocker	Channel	Working Concentration
Amiloride (72)	Epithelial Na^+ channel	10 μM
Carbenoxolone (73)	pannexin	100 μM
Gadolinium (III) chloride (74)	nonspecific	10 μM
MK-886 (75)	TRPM7	20 μM
ML-204 (76)	TRPC4	10 μM
RN1734 (67)	TRPV4	30 μM

In addition to specific blockers of mechanosensitive channels, nonspecific blockers of Ca^{2+} signaling were used during positive control experiments. EGTA, a selective chelator for Ca^{2+}, was used to remove Ca^{2+} from the media. The composition of Ca^{2+} free HBSS is given in Table 5.

Table 5. Composition of Ca^{2+}-free HBSS (0.1L).

Component	Mass	Molarity
NaCl (mw: 58.4 g/mol)	0.8 g	0.14 M
KCl (mw: 74.551 g/mol)	40 mg	0.005 M
EGTA (mw: 380.35 g/mol)	38.035 mg	0.001 M
$MgSO_4$-$7H_2O$ (mw: 246.475 g/mol)	10.0 mg	0.0004 M
$MgCl_2$-$6H_2O$ (mw: 203.303 g/mol)	10.0 mg	0.0005 M
Na_2HPO_4 (mw: 177.99 g/mol)	6.0 mg	0.0003 M
KH_2PO_4 (mw: 136.086 g/mol)	6.0 mg	0.0004 M
Glucose (mw: 180.156 g/mol)	0.1 g	0.006 M
$NaHCO_3$ (mw: 84.007 g/mol)	35 mg	0.004 M

Cell Fixation and Permeabilization

At the end of the 24 hour experimental period, both control and experimental cells in the silicone chambers were fixed for 15 min. using 3.7% paraformaldehyde in PBS. Cells were permeabilized for 20 min. with PBST (0.1% Triton X-100 in PBS) to enable penetration of the reagents in the EdU kit.

Fluorescence Labelling of S-Phase Cells

Cell proliferation is measured by identifying cells in S-phase of the cell cycle i.e. the DNA synthesis phase, using the Edu Click-iT® kit (Invitrogen). The EdU contains the alkyne and the Alexa Fluor® dye contains the azide. A click-chemistry reaction works, when a copper-catalyzed covalent reaction occurs between an azide and an alkyne. Additionally, standard aldehyde fixation and detergent based permeabilization are compulsory for the Click-iT® detection reagent. The detergent removes lipids and helps to increase access to the DNA for the two fluorescent stains. The Click-iT® EdU assay is useful to produce low background and high detection sensitivities. The components of the kit were assembled, used and stored according to manufacturer's instructions. A step by step protocol is provided in Appendix C.

Immunofluorescence and Image Analysis

Stained cells were visualized using widefield fluorescence microscopy with an Olympus BX-50 system (Cell Sens standard v1.14). The EdU labeled DNA was visualized using the TRITC filter cube while the Hoechst fluorescent DNA stain was visualized using the DAPI filter cube which has similar excitation and emission spectra. Images were processed and analyzed. Cells in S-phase, staining red, were compared to the total number of cells in a field of view, with blue, Hoechst-stained, nuclei. The ratio of S-phase cells to all cells in the fields of view were compared for the different treatments and a Students two-tailed t-test was used to assess statistical significance.

In-silico Identification of Mechanosensitive Channels in Human Keratinocytes

A human keratinocyte transcriptome (77) was downloaded, annotated and screened for mechanosensitive channels. The transcriptome screened human fibroblasts, melanocytes, and keratinocytes for 22582 genes from the human genome and reported at least one transcript for 19161 genes from 4 different screenings of human keratinocytes. Transcripts were arranged according to their reads per kilobase of transcript per million mapped reads (RPKM), a normalized unit of transcript expression. The BioMart program was then used to identify the gene name for all the ensemble identifiers. First, all channels were sorted from the large list of transcripts. Second, MSCs s were and Ca^{2+} permeable channels were extracted and listed from highest RPKM to lowest RPKM in Table 6.

RESULTS

Identification of Mechanosensitive Channels in Human Keratinocytes

Stretch-induced cellular proliferation in keratinocytes requires Ca^{2+} influx. In order to identify the most abundant mechanosensitive ion channels in human keratinocytes and other mechanosensitive, Ca^{2+}-dependent pathways, a human keratinocyte transcriptome (77) was downloaded and screened for the transcripts of interest. The transcriptome listed 22,582 transcripts from human keratinocytes according to reads per kilobase of transcript, per million mapped reads (RPKM) a relative measure of transcript quantity.

309 out of 22,582 transcripts are identified as membrane channels permeable to Na^+, K^+, Ca^{2+}, Cl^-, Zn^{2+}, H^+, water (aquaporins) and small organics. Furthermore, 91 transcripts out of the 309 are transcripts for Ca^{2+} permeable channels, their associated proteins, and associated factors. Transcripts for MSCs, Ca^{2+} permeable channels, their associated proteins, and associated factors are arranged in order of most abundant transcript to least abundant in Table 6 below for RPKM values ≥ 0.5. An extension of Table 6 is listed in Appendix D for transcripts with lower RPKM values. According to this list TRPM7, Piezo1, TRPV3, polycystic 2 (TRPP2), polycystic 1 (TRPP1), TRPM8, TRPM1, TRPV2, TRPM4 and the epithelial Na^+ channel have RPKM values greater than 1. A transcript for Pannexin 1, a mechanosensitive ATP release channel which activates purinergic receptors is the 2nd most abundant. Numerous purinergic channels are present including P2X4, P2X7, P2Y1 and P2Y11. Therefore, activation of pannexin which releases ATP could increase Ca^{2+} influx through purinergic receptors. These influx pathways will be tested to determine their relevance in keratinocyte proliferation.

Table 6. Transcripts for Ca^{2+} influx pathways.

Ensemble ID	Annotation	Transcript (RPKM)
ENSG00000092439	transient receptor potential cation channel subfamily M member 7 [Acc:HGNC:17994]	14.2
ENSG00000110218	pannexin 1 [Acc:HGNC:8599]	9.5
ENSG00000103335	piezo type mechanosensitive ion channel component 1 [Acc:HGNC:28993]	3.7
ENSG00000196557	calcium voltage-gated channel subunit alpha1 H [Acc:HGNC:1395]	3.5
ENSG00000167723	transient receptor potential cation channel subfamily V member 3 [Acc:HGNC:18084]	3.3
ENSG00000118762	polycystin 2, transient receptor potential cation channel [Acc:HGNC:9009]	3.0
ENSG00000008710	polycystin 1, transient receptor potential channel interacting [Acc:HGNC:9008]	2.7
ENSG00000135124	purinergic receptor P2X4 [Acc:HGNC:8535]	2.3
ENSG00000198420	TRPM8 channel associated factor 1 [Acc:HGNC:22201]	2.1
ENSG00000107614	polycystin 2 like 1, transient receptor potential cation channel [Acc:HGNC:9011]	1.6
ENSG00000134160	transient receptor potential cation channel subfamily M member 1 [Acc:HGNC:7146]	1.6
ENSG00000187688	transient receptor potential cation channel subfamily V member 2 [Acc:HGNC:18082]	1.6
ENSG00000130529	transient receptor potential cation channel subfamily M member 4 [Acc:HGNC:17993]	1.3
ENSG00000111319	sodium channel epithelial 1 alpha subunit [Acc:HGNC:10599]	1.2
ENSG00000089041	purinergic receptor P2X 7 [Acc:HGNC:8537]	1.1
ENSG00000169860	purinergic receptor P2Y1 [Acc:HGNC:8539]	1.0
ENSG00000167535	calcium voltage-gated channel auxiliary subunit beta 3 [Acc:HGNC:1403]	0.9
ENSG00000160325	calcium channel flower domain containing 1 [Acc:HGNC:1365]	0.8
ENSG00000168447	sodium channel epithelial 1 beta subunit [Acc:HGNC:10600]	0.8
ENSG00000144935	transient receptor potential cation channel subfamily C member 1 [Acc:HGNC:12333]	0.8
ENSG00000078795	polycystin 2 like 2, transient receptor potential cation channel [Acc:HGNC:9012]	0.5
ENSG00000244165	purinergic receptor P2Y11 [Acc:HGNC:8540]	0.5
ENSG00000170379	TRPM8 channel associated factor 2 [Acc:HGNC:26878]	0.5

Tensile Stress Promotes Keratinocyte Proliferation

Cell proliferation of a clonal, human epidermal keratinocyte cell line (HaCaT) was monitored during application of tensile stress. Proliferation was monitored under stretched and unstretched conditions. Under stretched conditions keratinocytes were subjected to one-dimensional tensile stress by increasing their length by 10% on silicone chambers for 24 h. Control cells were grown on the same silicone chambers without stretch. Cell proliferation was quantitated by monitoring EdU incorporation during the last 3 hours of experimentation.

Four independent unstretched chambers were seeded with HaCaTs, (Figure 4A). After the experimental incubation period, cells were fixed and the EdU was stained with the Click-IT method (Figure 4B) to identify cells in the proliferative state and all nuclei were stained with Hoechst (Figure 4C), in order to count all cells in the field of view. The proliferation rate (number of EdU labeled cells/ Hoechst labeled cells) was normalized to 100% (Figure 5). Stretching of six independent silicone chambers, seeded with HaCaTs, increased the number of cells in S-phase to 198% compared to the unstretched controls (Figure 5), with a high statistical significance ($p < 0.0001$).

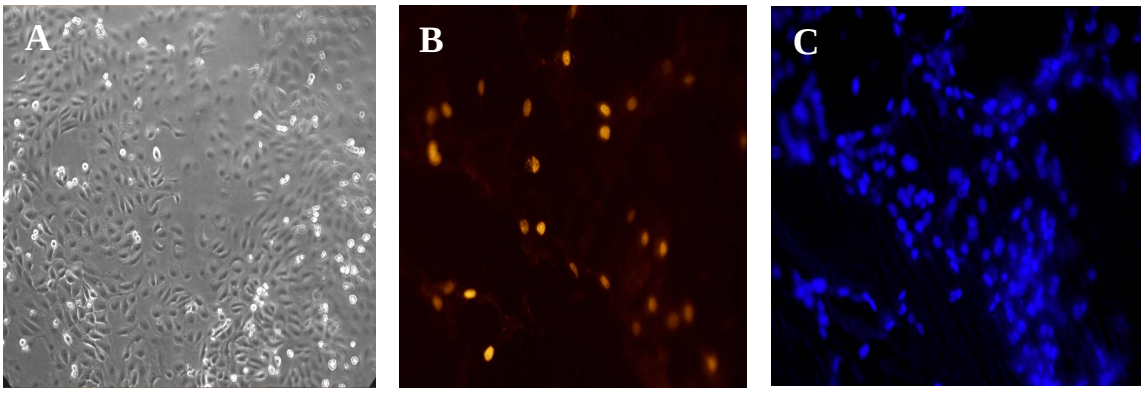

Figure 4. Images of human keratinocytes and labelled keratinocyte nuclei. **(A)** HaCaT cells, visualized with phase contrast, adhere well to the collagen-functionalized silicone chambers. **(B)** EdU incorporated into the nuclei was stained with Alexa Fluor 555. **(C)** Hoechst 33342 was used to stain all cellular nuclei. The images in B and C are collected from the same chamber.

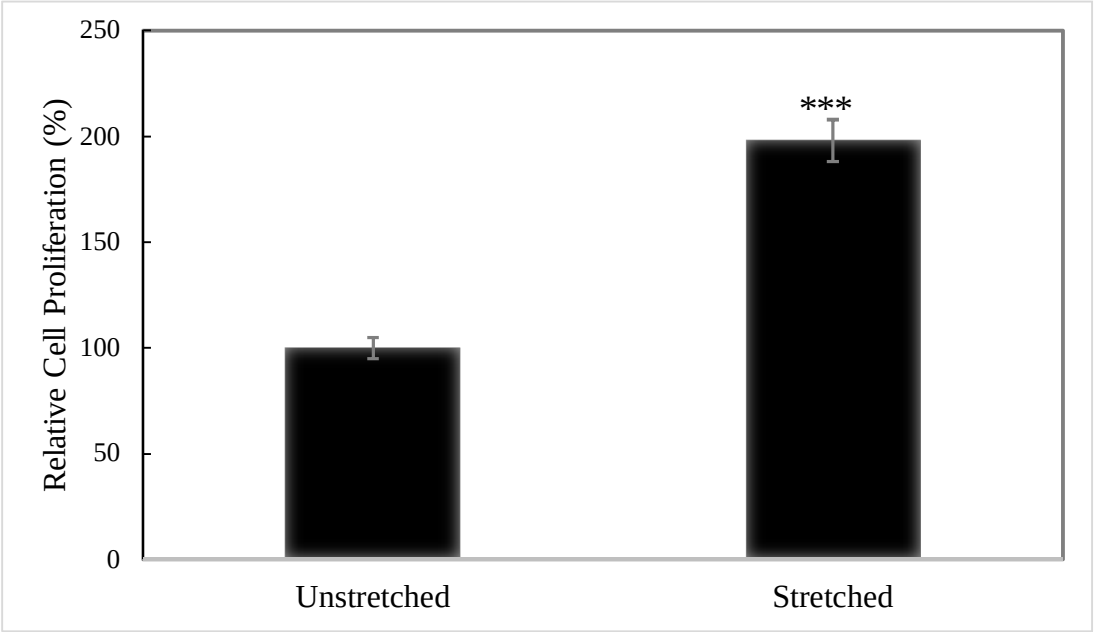

Figure 5. Stretching cells promotes the proliferative state. Stretching cells by 10% of their initial length, places twice as many cells in the proliferative state compared to unstretched conditions. (*** = $p < 0.0001$).

Stretch-Induced Proliferation Requires Ca^{2+} Influx

Previous studies have indicated that Ca^{2+} influx is required for cellular proliferation (68, 78-80). We tested these former results in order to confirm them in our system (Figure 6). Ca^{2+} was removed from the extracellular medium by first not adding it to the culture media and second by buffering any remaining Ca^{2+} with EGTA (1mM). Ca^{2+} influx through plasma membrane Ca^{2+} channels was blocked with the non-selective channel blocker gadolinium (10 μM). In the presence of normal extracellular Ca^{2+}, stretched cells proliferated nearly 2-fold greater than unstretched cells (Figure 6). However, reduced extracellular Ca^{2+} (EGTA), reduced proliferation ($p < 0.02$). By blocking Ca^{2+} influx with the Ca^{2+} channel blocker, Gd^{3+}, proliferation was also impaired (Figure 6, $p < 0.001$).

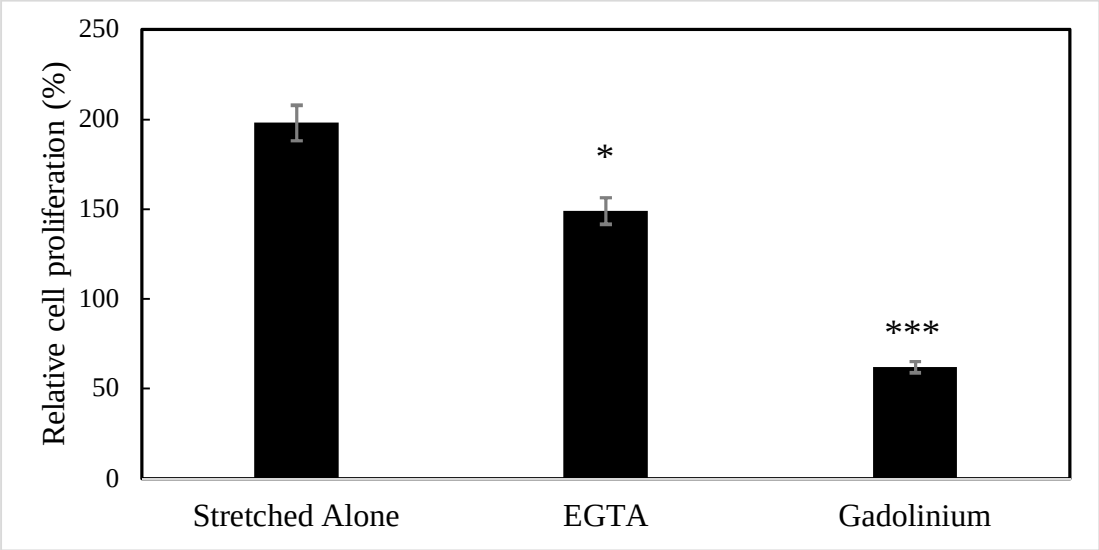

Figure 6. Impairing Ca^{2+} influx reduces proliferation of stretched cells. Removing extracellular Ca^{2+} and buffering remaining Ca^{2+} with EGTA significantly reduced proliferation. The non-selective Ca^{2+} channel blocker, Gd^{3+}, also impaired proliferation. (* = $p < 0.05$, *** = $p < 0.001$)

DMSO Reduces Proliferation

DMSO is an amphiphilic solvent that promotes solubilization of hydrophobic pharmacological agents. It was required to dissolve some of the pharmacological agents in the culture media. However, 0.1% DMSO, a low concentration that normally does not affect cell function, impaired proliferation of HaCaTs. In the presence of 10% stretch and 0.1% DMSO (Figure 7), proliferation was no greater than in the unstretched state.

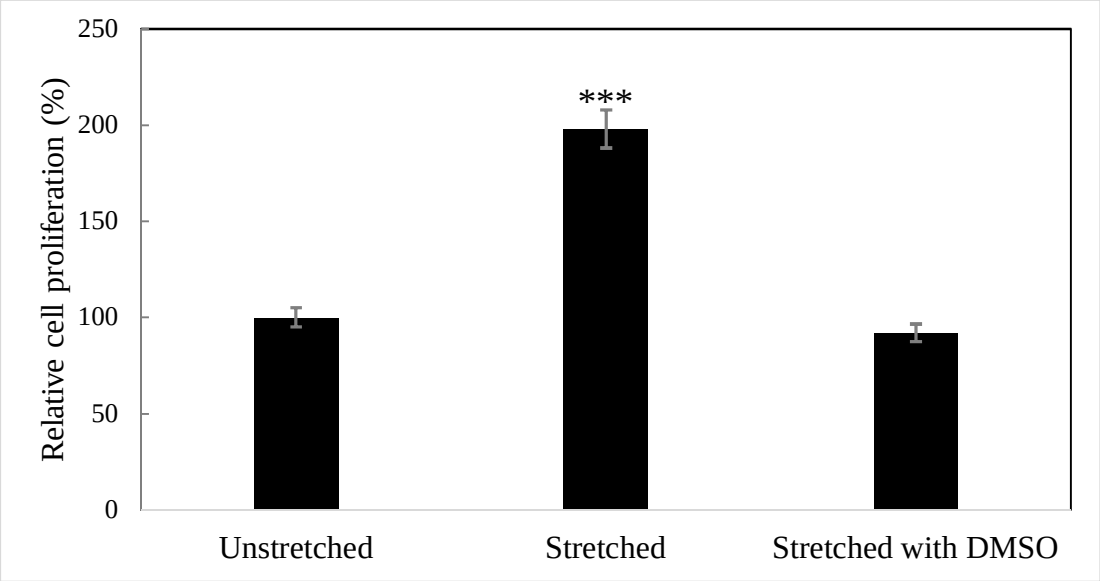

Figure 7. DMSO decreases stretch-activated proliferation. 0.1% DMSO completely nullifies the increased proliferation due to 10% stretch. (*** = $p < 0.001$)

Pharmacological agents with high selectivity for blocking specific mechanosensitive, Ca^{2+} permeable channels were selected to block Ca^{2+} influx and assess proliferation in the stretched state. 0.1% DMSO was used as a control but did have a dramatic effect on cells itself, as noted above. Stock solutions of amiloride, RN1734, ML204 and MK-886 were dissolved in DMSO. Final concentrations of the compounds

were used that are known to block greater than 90% of the channels including amiloride (10 μM), RN1734 (30 μM), MK886 (20 μM), ML204 (10 μM). However, when compared to the 0.1% DMSO control itself, none of the pharmacological agents caused statistically significant reduction in the proliferation in the 10% stretched condition.

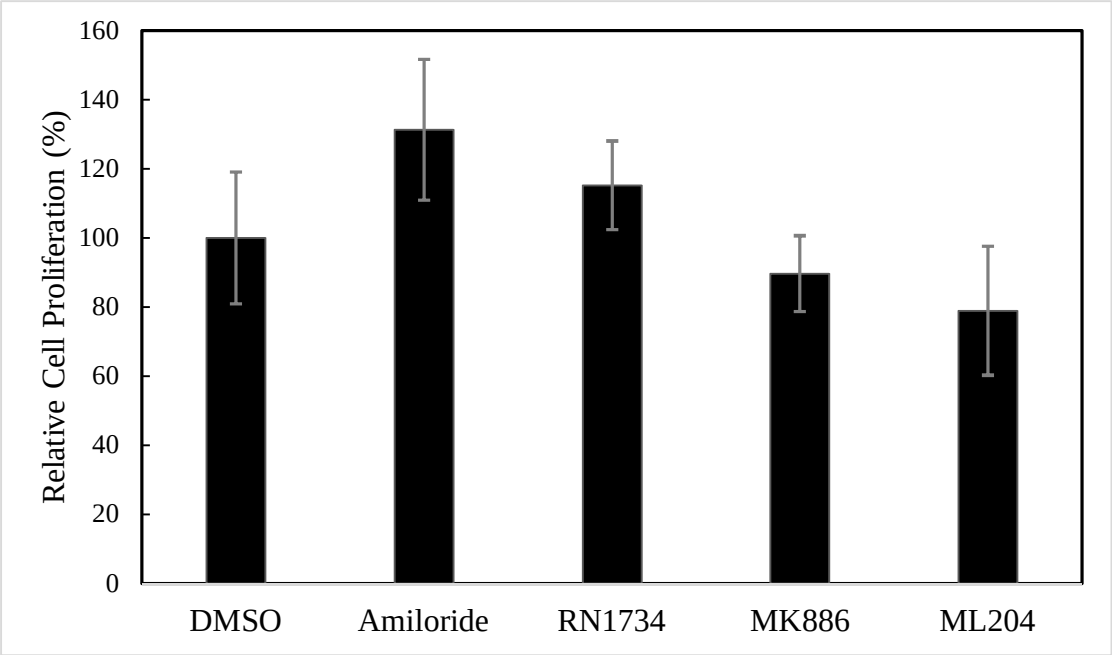

Figure 8. Effect of pharmacological drugs and DMSO on HaCaT proliferation. When compared to DMSO neither amiloride, blocker of the epithelial Na^+ channel, nor RN1734, blocker of TRPV4, nor MK886, blocker of TRPM7, nor ML204, blocker of TRPC4 inhibited proliferation.

Pharmacological inhibition of pannexin 1, the channel with the 2nd greatest RPKM in human keratinocytes, Table 6, was performed with 100 μM carbenoxolone in the absence of DMSO, as it is a hydrophilic compound. Pannexin 1 is an ATP release

channel. Released ATP can activate Ca^{2+} influx through local purinergic channels which are also present in Table 6. Carbenoxolone significantly impaired cellular proliferation in response to 10% stretch.

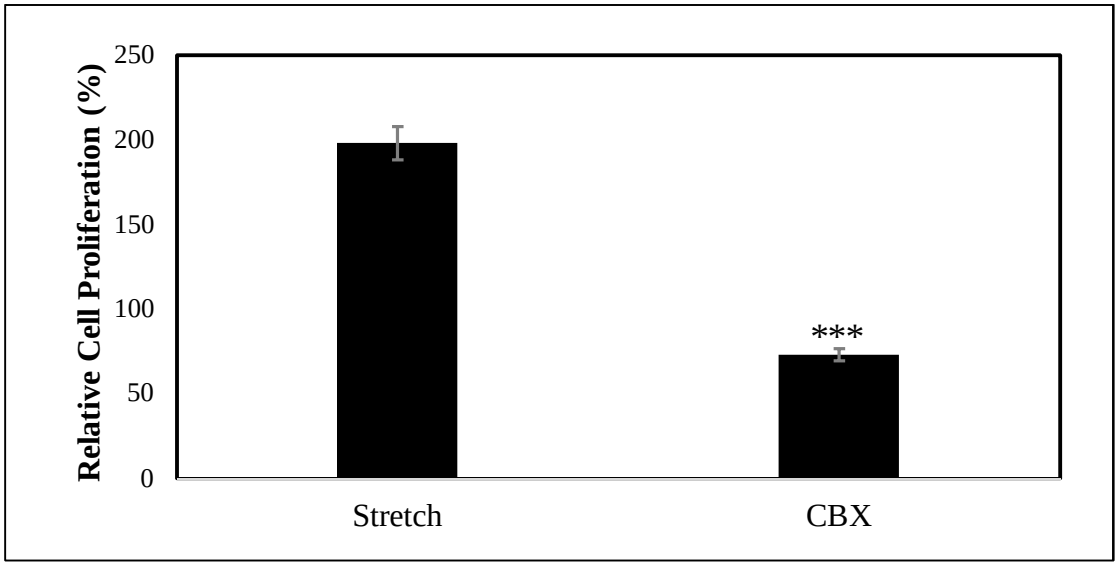

Figure 9. Blocking the pannexin channel inhibits cell proliferation. ($p < 0.001$).

DISCUSSION

Human keratinocytes are highly sensitive to tensile stress and respond by increasing DNA synthesis in preparation for cell division, to reduce the tensile stress. As a result, tensile stress induces cell proliferation as shown earlier (68, 70). We confirm that continuous mechanical stretching of keratinocytes by +10% for 24 hrs. significantly promotes DNA replication when compared to unstretched controls, Fig. 5, ($p < 0.0001$). In the stretched condition, the number of cells in S-phase during the final 3 hours of stretching, monitored by using EdU incorporation in HaCaT nuclei, nearly doubled compared to unstretched controls.

Calcium channel activation on the cell membrane and calcium influx is crucial for promoting cellular proliferation especially under the stretched condition (68, 70). In order to confirm these earlier reports and assess the reliability of our setup, we impaired Ca^{2+} influx by removing it from the medium and by using a non-selective Ca^{2+} channel blocker, Gd^{3+}. The Ca^{2+} reaction was significantly inhibited in Ca^{2+}-free solution (1 mM EGTA), although not as much as anticipated. Under these conditions the free Ca^{2+} concentration can only be estimated and no Ca^{2+} concentration measurements were performed. Reducing extracellular Ca^{2+} even further with 2 mM EGTA may provoke a larger response. The addition of Gd^{3+} (10 μM), in the stretched state, reduced proliferation to about 65% of the proliferation in the unstretched state. We conclude that increased HaCaT proliferation due to stretch is dependent on Ca^{2+} influx from the extracellular medium.

In order to assess the Ca^{2+} influx pathway which leads to proliferation, we collected a human keratinocyte transcriptome, identified all of the transcripts and filtered

the transcripts in 2 steps: first, identification of all plasma membrane channels, second, identification of all channels with Ca^{2+} permeability or that were linked to mechanosensitive Ca^{2+} influx. That list, shown in Table 6 was used to select the channels with the highest RPKM values as we hypothesize that those would have the greatest impact on cellular function if they were impaired. Table 6 was used only as a guide as protein levels are not directly proportional to transcript levels.

We performed pharmacological inhibition of some of the top channels in Table 4, including TRPM7 (RPKM 14.2) and pannexin (RPKM 9.5) and other channels commonly found in keratinocytes for which pharmacological inhibitors were commercially available including epithelial Na^{+} channels, alpha subunit (RPKM 1.2) and beta subunit (RPKM 0.8) and TRPV4 which is closely related to TRPV3 (RPKM 3.3) and TRPV2 (RPKM 1.6). Unfortunately, there is no specific inhibitor for the mechanosensitive channel Piezo 1 which had the 3rd largest RPKM value in keratinocytes.

Most of the blockers had hydrophobic properties and were dissolved in DMSO to increase their solubility in aqueous media. When we assessed the influence of DMSO on cellular proliferation we were surprised to learn that it suppressed cell proliferation at the low concentration of 0.1%. We hypothesize that DMSO may have influenced proliferation by reducing stretch in the membrane. DMSO is lipophilic and therefore partitions within the plasma membrane. The 10% stretch of the plasma membrane may have been offset by the inclusion of the DMSO into the membrane, thus decreasing tension in the membrane and reducing channel activation. This hypothesis should be tested further.

Pharmacological inhibition of TRPM7, TRPV4, TRPC4 and ENaC had no effect on proliferation in comparison to the DMSO control, which was used as a carrier for these compounds. By contrast, inhibition of pannexin by CBX, had a significant affect in inhibiting proliferation. Pannexin however, is not a mechanosensitive Ca^{2+} channel. It is a mechanosensitive ATP release channel (80-83). ATP is known to promote cellular proliferation in other cell types (84-86). In keratinocytes, ATP release by pannexin channels can activate purinergic channels which are also found in keratinocytes as indicated by Table 6. P2X4 and P2X7 are ligand gated Ca^{2+} permeable channels that open in response to extracellular ATP (61, 87, 88). The P2Y1 and P2Y11 channels are also activated by ATP and lead to a rise in intracellular Ca^{2+} (89, 90).

We hypothesize that mechanotransduction promotes proliferation of human epidermal keratinocytes by activating an ATP channel, pannexin, which promotes a rise in intracellular Ca^{2+}. Considering that our hypothesis involves purinergic channels, we can further test our hypothesis by blocking the purinergic receptors with known inhibitors. These experiments could be followed up by performing concentration dependent response curves for the channel blockers and possibly by performing channel knockdown experiments to remove critical proteins involved with the stretch-induced proliferation pathway.

These results are useful for explaining the changes made by tensile stress in keratinocytes during wound healing. The epidermis makes use of tensile stress to determine whether more or fewer cells are required to cover the entire body. Increased tensile stress indicates an epidermis with a larger surface area is required while less stress indicates a lower surface area is required and cells are extruded from the epithelium (91).

By identifying pharmacological activators of this mechanosensitive pathway, we could speed wound healing by promoting proliferation of the cells to cover the wound bed. This study also helps to clarify the role of the multiple different Ca^{2+} permeable channels in human keratinocytes.

LITERATURE CITED

1. Millington, P.F. and R. Wilkinson, *Skin (Digitally printed version ed.).* Cambridge University Press., 2009. **ISBN 978-0-521-10681-8.**: p. 49–50.
2. *Skin care" (analysis).* Health-Cares.net, 2007. http://skin-care.health-cares.net/oily-skin-care.php.
3. Aguirre, D.C., *Understanding Male Skin.* Dermascope Magazine, 2015.
4. Gawkrodger, D.J., *Dermatology: An Illustrated Text.* Churchill Livingston, 1998. **2nd**.
5. MD., K., *Introduction: Moist wound healing.* American Journal of Surgery, 1994. **167**((1A Suppl)): p. 1S–6S.
6. E, M., W. P, and M. J., *The Integumentary System. Human Anatomy.* . Textbook, 2014: p. 105.
7. KS, S., *Human Anatomy: The Unity of Form and Function.* McGraw Hill Education 2007. **4th edition**.
8. James, W., T. Berger, and D. Elston, *Andrews' Diseases of the Skin: Clinical Dermatology* Saunders, 10th ed., 2005. **ISBN-10: 1437703143**: p. 2-3.
9. Fawcett, D.W., *Bloom and Fawcett: a textbook of histology*. 1986.
10. Sanders, J.E., B.S. Goldstein, and D.F. Leotta, *Skin response to mechanical stress: adaptation rather than breakdown-a review of the literature.* Journal of Rehabilitation Research and Development, 1995. **32**: p. 214-214.
11. Mustoe, T., *Dermal ulcer healing: Advances in understanding.* Tissue repair and ulcer/wound healing: molecular mechanisms, therapeutic targets and future directions. Paris, France: EUROCONFERENCES, 2005: p. 17-18.

12. Snyder, R.J., *Treatment of nonhealing ulcers with allografts.* Clinics in Dermatology, 2005. **23**(4): p. 388-395.

13. Han, G. and R. Ceilley, *Chronic wound healing: a review of current management and treatments.* Advances in Therapy, 2017. **34**(3): p. 599-610.

14. Mathieu, D., *Handbook on hyperbaric medicine*. Vol. 27. 2006: Springer.

15. Hess, C.T., *Checklist for factors affecting wound healing.* Advances in Skin & Wound Care, 2011. **24**(4): p. 192.

16. Baranoski, S. and E.A. Ayello, *Wound care essentials: Practice principles*. 2008: Lippincott Williams & Wilkins.

17. FLYNN, J., *Understanding chronic wound management: part I.* Pharmaceutical Journal, 2009. **282**(7558): p. 777-780.

18. Rushton, I., *Understanding the role of proteases and pH in wound healing.* Nursing Standard (through 2013), 2007. **21**(32): p. 68.

19. Nunan, R., K.G. Harding, and P. Martin, *Clinical challenges of chronic wounds: searching for an optimal animal model to recapitulate their complexity.* Disease Models & Mechanisms, 2014. **7**(11): p. 1205-1213.

20. Eming, S.A., T. Krieg, and J.M. Davidson, *Inflammation in wound repair: molecular and cellular mechanisms.* Journal of Investigative Dermatology, 2007. **127**(3): p. 514-525.

21. Harding, K. and R. Edwards, *Bacteria and wound healing vol. 17*. 2004, United States: Lippincott Williams & Wilkins.

22. Wolcott, R.D., D.D. Rhoads, and S.E. Dowd, *Biofilms and chronic wound inflammation.* Journal of Wound Care, 2008. **17**(8): p. 333-341.

23. Woo, K., E.A. Ayello, and R.G. Sibbald, *The edge effect: current therapeutic options to advance the wound edge.* Advances in Skin & Wound Care, 2007. **20**(2): p. 99-117.

24. Stojadinovic, A., et al., *Topical advances in wound care.* Gynecologic Oncology, 2008. **111**(2): p. S70-S80.

25. Attinger, C.E., et al., *Clinical approach to wounds: debridement and wound bed preparation including the use of dressings and wound-healing adjuvants.* Plastic and Reconstructive Surgery, 2006. **117**(7S): p. 72S-109S.

26. Brownrigg, J., et al., *Evidence-based management of PAD & the diabetic foot.* European Journal of Vascular and Endovascular Surgery, 2013. **45**(6): p. 673-681.

27. Richmond, N.A., A.D. Maderal, and A.C. Vivas, *Evidence-based management of common chronic lower extremity ulcers.* Dermatologic Therapy, 2013. **26**(3): p. 187-196.

28. Ramsey, S.D., et al., *Incidence, outcomes, and cost of foot ulcers in patients with diabetes.* Diabetes Care, 1999. **22**(3): p. 382-387.

29. *Optimal Care of Chronic, Non-Healing, Lower Extremity Wounds: A Review of Clinical Evidence and Guidelines.* Canadian Agency for Drugs and Technologies in Health, 2013. **Rapid Response Report: Summary with Critical Appraisal**(Ottawa (ON)).

30. Demidova-Rice, T.N., M.R. Hamblin, and I.M. Herman, *Acute and impaired wound healing: pathophysiology and current methods for drug delivery, part 1: normal and chronic wounds: biology, causes, and approaches to care.* Advances in Skin & Wound Care, 2012. **25**(7): p. 304.

31. Etufugh, C.N. and T.J. Phillips, *Venous ulcers.* Clinics in Dermatology, 2007. **25**(1): p. 121-130.

32. Sieggreen, M.Y. and R.A. Kline, *Arterial insufficiency and ulceration: diagnosis and treatment options.* Advances in Skin & Wound Care, 2004. **17**(5): p. 242-251.

33. Reiber, G.E., *Diabetic foot care. Financial implications and practice guidelines.* Diabetes Care, 1992. **15**: p. 29-31.

34. Reddy, M., S.S. Gill, and P.A. Rochon, *Preventing pressure ulcers: a systematic review.* Journal of the American Medical Association, 2006. **296**(8): p. 974-984.

35. Gosain, A. and L.A. DiPietro, *Aging and wound healing.* World Journal of Surgery, 2004. **28**(3): p. 321-326.

36. Narayan, K.V., et al., *Lifetime risk for diabetes mellitus in the United States.* Journal of the American Medical Association, 2003. **290**(14): p. 1884-1890.

37. Shankaran, V., M. Brooks, and E. Mostow, *Advanced therapies for chronic wounds: NPWT, engineered skin, growth factors, extracellular matrices.* Dermatologic Therapy, 2013. **26**(3): p. 215-221.

38. Nieto, M.A., et al., *EMT: 2016.* Cell, 2016. **166**(1): p. 21-45.

39. Jaalouk, D.E. and J. Lammerding, *Mechanotransduction gone awry.* Nature Reviews Molecular Cell Biology, 2009. **10**(1): p. 63.

40. Ingber, D., *Mechanobiology and diseases of mechanotransduction.* Annals of Medicine, 2003. **35**(8): p. 564-577.

41. Sukharev, S. and F. Sachs, *Molecular force transduction by ion channels–diversity and unifying principles.* Journal of Cell Science, 2012. **125**(13): p. 3075-3083.

42. Gottlieb, P.A. and F. Sachs, *Cell biology: The sensation of stretch.* Nature, 2012. **483**(7388): p. 163.

43. Thompson, W.R., et al., *Understanding mechanobiology: physical therapists as a force in mechanotherapy and musculoskeletal regenerative rehabilitation.* Physical Therapy, 2016. **96**(4): p. 560-569.

44. Reichelt., J., *Mechanotransduction of keratinocytes in culture and in the epidermis.* European Journal of Cell Biology, 2003. **86**(2003): p. 807-816.

45. Cadart, C., et al., *Exploring the function of cell shape and size during mitosis.* Developmental Cell, 2014. **29**(2): p. 159-169.

46. Fink, J., et al., *External forces control mitotic spindle positioning.* Nature cell Biology, 2011. **13**(7): p. 771.

47. Ranft, J., et al., *Fluidization of tissues by cell division and apoptosis.* Proceedings of the National Academy of Sciences, 2010 USA, **107**(49):20863-8.

48. Davies, P.F., *Flow-mediated endothelial mechanotransduction.* Physiological Reviews, 1995. **75**(3): p. 519-560.

49. Sachs, F., *Stretch-activated ion channels: what are they?* Physiology, 2010. **25**(1): p. 50-56.

50. Bowman, C.L., et al., *Mechanosensitive ion channels and the peptide inhibitor GsMTx-4: history, properties, mechanisms and pharmacology.* Toxicon, 2007. **49**(2): p. 249-270.

51. Suchyna, T.M. and F. Sachs, *Mechanosensitive channel properties and membrane mechanics in mouse dystrophic myotubes.* The Journal of Physiology, 2007. **581**(1): p. 369-387.

52. Markin, V. and F. Sachs, *Thermodynamics of mechanosensitivity.* Current Topics in Membranes, 2007. **58**: p. 87-119.

53. Sukharev, S., et al., *Two types of mechanosensitive channels in the Escherichia coli cell envelope: solubilization and functional reconstitution.* Biophysical Journal, 1993. **65**(1): p. 177-183.

54. Dedman, et al., *The mechano-gated K2P channel TREK-1.* European Biophysics Journal, 2008. **38**(3): p. 293–303.

55. Lumpkin, E.A. and M.J. Caterina, *Mechanisms of sensory transduction in the skin.* Nature, 2007. **445**(7130): p. 858.

56. Sachs, F. and C.E. Morris, *Mechanosensitive ion channels in nonspecialized cells*, in *Reviews of Physiology Biochemistry and Pharmacology, Volume 132*. 1998, Springer. p. 1-77.

57. Hamill, O.P. and B. Martinac, *Molecular basis of mechanotransduction in living cells.* Physiological Reviews, 2001. **81**(2): p. 685-740.

58. Sackin, H., *Mechanosensitive channels.* Annual Review of Physiology, 1995. **57**: p. 333–53.

59. ME, D.V., et al., *Mechanosensory neurons, cutaneous mechanoreceptors, and putative mechanoproteins.* Microscopy Research and Technique, 2012. **75**(8): p. 1033–43.

60. Coste, B., et al., *Piezo1 and Piezo2 Are Essential Components of Distinct Mechanically Activated Cation Channels.* Science, 2010. **330**(6000): p. 55-60.

61. North, R.A., *Molecular physiology of P2X receptors.* Physiological Reviews, 2002. **82**(4): p. 1013-1067.

62. Markin, V. and B. Martinac, *Mechanosensitive ion channels as reporters of bilayer expansion. A theoretical model.* Biophysical Journal, 1991. **60**(5): p. 1120-1127.

63. Perozo, E., et al., *Open channel structure of MscL and the gating mechanism of mechanosensitive channels.* Nature, 2002. **418**(6901): p. 942.

64. Hamill, O.P. and D.W. McBride, *Rapid adaptation of single mechanosensitive channels in Xenopus oocytes.* Proceedings of the National Academy of Sciences USA, 1992. **89**(16): p. 7462-7466.

65. Chen, N.X., et al., *Ca2+ regulates fluid shear-induced cytoskeletal reorganization and gene expression in osteoblasts.* American Journal of Physiology-Cell Physiology, 2000. **278**(5): p. C989-C997.

66. Cotrina, M.L., et al., *Connexins regulate calcium signaling by controlling ATP release.* Proceedings of the National Academy of Sciences USA, 1998. **95**(26):15735-15740.

67. Nilius, B., et al., *TRPV4 calcium entry channel: a paradigm for gating diversity.* American Journal of Physiology-Cell Physiology, 2004. **286**(2): p. C195-C205.

68. Shoichiro Yano, et al., *Mechanical Stretching In Vitro Regulates Signal Transduction Pathways and Cellular Proliferation in Human Epidermal Keratinocytes.* Journal of Investigative Dermatology, 2004. **122**(2004): p. 783 – 790.

69. Koh, K.-S., et al., *Quantitative studies on PDMS-PDMS interface bonding with piranha solution and its swelling effect.* Micromachines, 2012. **3**(2): p. 427-441.

70. Kippenberger, S., et al., *Signaling of mechanical stretch in human keratinocytes via MAP kinases*, in *Journal of Investigative Dermatology*. 2000. p. 408-12.

71. Renò, F., V. Traina, and M. Cannas, *Mechanical stretching modulates growth direction and MMP-9 release in human keratinocyte monolayer.* Cell Adhesion & Migration, 2009. **3**(3): p. 239-242.

72. Kleyman, T.R. and E.J. Cragoe, *Amiloride and its analogs as tools in the study of ion transport.* The Journal of Membrane Biology, 1988. **105**(1): p. 1-21.

73. Michalski, K. and T. Kawate, *Carbenoxolone inhibits Pannexin1 channels through interactions in the first extracellular loop.* The Journal of General Physiology, 2016. **147**(2): p. 165-174.

74. Yang, X.-c. and F. Sachs, *Block of stretch-activated ion channels in Xenopus oocytes by gadolinium and calcium ions.* Science, 1989. **243**(4894): p. 1068-1071.

75. Chen, H.-C., et al., *Blockade of TRPM7 channel activity and cell death by inhibitors of 5-lipoxygenase.* PLoS One, 2010. **5**(6): p. e11161.

76. Miller, M.R., et al., *Novel chemical inhibitor of TRPC4 channels.* 2011.

77. Reemann, P., E. Reimann, and *Melanocytes in the skin – comparative whole transcriptome analysis of main skin cell types.* PLoS One, 2014. **9**(12).

78. Capiod, T., *Cell proliferation, calcium influx and calcium channels.* Biochimie, 2011. **93**(12):2075-2079..

79. Capiod, T., *The need for calcium channels in cell proliferation.* Recent Patents On Anti-Cancer Drug Discovery, 2013. **8**(1): p. 4-17.

80. Takada, H., K. Furuya, and M. Sokabe, *Mechanosensitive ATP release from hemichannels and Ca(2)(+) influx through TRPC6 accelerate wound closure in keratinocytes.* Journal of Cell Science 2014. **127**(Pt 19): p. 4159-71.

81. Dahl, G. and S. Locovei, *Pannexin: To Gap or not to Gap, is that a Question?* International Union of Biochemistry and Molecular Biology Life, 2006. **58**(7): p. 409 – 419.

82. Michael T. Barbe, Hannah Monyer, and R. Bruzzone, *Cell-Cell Communication Beyond Connexins: The Pannexin Channels.* PHYSIOLOGY, 2006. **21**(2): p. 103–114.

83. Burrell, H.E., et al., *Human keratinocytes release ATP and utilize three mechanisms for nucleotide interconversion at the cell surface.* Journal of Biological Chemistry, 2005. **280**(33): p. 29667-76.

84. SR1, B., et al., *Pannexin 3 is a novel target for Runx2, expressed by osteoblasts and mature growth plate chondrocytes.* Journal of Bone and Mineral Research (JBMR) 2011. **26**(12): p. 2911-22.

85. Burnstock, G., *Purinergic signaling and vascular cell proliferation and death.* Arteriosclerosis, Thrombosis, and Vascular Biology, 2002. **22**(3): p. 364-373.

86. Jiang, L.-H., et al., *ATP-induced Ca 2+-signalling mechanisms in the regulation of mesenchymal stem cell migration.* Cellular and Molecular Life Sciences, 2017. **74**(20): p. 3697-3710.

87. Khakh, B.S. and R.A. North, *Neuromodulation by extracellular ATP and P2X receptors in the CNS.* Neuron, 2012. **76**(1): p. 51-69.

88. Guo, C., et al., *Evidence for functional P2X4/P2X7 heteromeric receptors.* Molecular Pharmacology, 2007 **72**(6):1447-1456.

89. Burrell, H.E., et al., *Human keratinocytes express multiple P2Y-receptors: evidence for functional P2Y1, P2Y2, and P2Y4 receptors.* Journal of Investigative Dermatology, 2003. **120**(3): p. 440-447.

90. Erb, L. and G.A. Weisman, *Coupling of P2Y receptors to G proteins and other signaling pathways.* Wiley Interdisciplinary Reviews: Membrane Transport and Signaling, 2012. **1**(6): p. 789-803.

91. Eisenhoffer, G.T., et al., *Crowding induces live cell extrusion to maintain homeostatic cell numbers in epithelia.* Nature, 2012. **484**(7395): p. 546.

APPENDIX A

This appendix lists the full composition of DMEM culture medium and the stock solutions of pharmacological inhibitors used in the experiments. All the media was sterile filtered and kept in refrigerator at 2-8 °C. Stock solutions were also kept at 2-8 °C

Table 7. Composition of DMEM culture medium.

Component	Amount	Concentration
DMEM (Gibco™ DMEM)	1 packet	High Glucose
DI H_2O	1000 mL	
FBS	100 mL	10%
$NaHCO_3$ (mw: 84.007 g/mol)	3.7 g	
Pen-strep	10 mL	10,000 U/mL

Table 8. Stock solutions of pharmacological inhibitors.

Blockers	Amount	Solvent
Amiloride	5 mg	1.88 mL DMSO
ML-204	2.26 mg	1 mL DMSO
CBX	0.615mg	1 mL Hank's Medium
Gd^{+3}	26.36 mg	1 mL water
MK-886	2.36 mg	250 µL DMSO
RN1734	0.6	DMSO

APPENDIX B

This appendix describes the step by step protocol for the preparation of the silicone chambers and surface modification of chambers

Preparation of silicon chambers:

SYLGARD ® 184 Silicone elastomer kit is used to prepare the PDMS chambers.

1. Weight the base and curing reagents in [10: 0.86 (w/w)].
2. Mix them well for 10-15 sec.
3. Pour the mixture into the chamber molds
4. The mixture was degassed at room temperature for 2-3 hrs. within chamber molds.
5. Chamber molds were baked at 37°C for overnight in dry hot air oven.
6. Chambers must be at room temperature for 30 mins.
7. Gently take the chambers off from the chamber mold.
8. Keep them in clean and dry place.

Protocol for surface modification of chambers

1. Measure Conc. (90%) Sulfuric acid and (30%) Hydrogen peroxide in 3:1 ratio carefully.
2. Carefully, mixing the Conc. H_2SO_4 and 30 % H_2O_2 together. This mixture produces heat at room temperature and generate an exothermic reaction.
3. Allow the mixture to cool down at room temperature before applying on chambers.
4. Cured PDMS chambers were treated with piranha solution for 2 mins at room temperature and washed with water.
5. Soaking the chambers will get better cell adhesion on the chambers.

6. Chambers were filled with DI water.
7. Keep the chambers in the same stages for 10 mins.
8. Repeat the same process twice to remove the proper chemicals from the chambers.

APPENDIX C

This appendix describes the methods for using the Click-iT® EDU Alexa Fluor 555 Imaging kit solution. All the vials must be at room temperature before opening and all the stock solution must keep at deep freezer or refrigerator.

Table 9. Stock solutions of Click-iT® kit components.

Name	Component	Solvent
10 mM EdU	A	2 mL DMSO
Alexa Fluor® azide	B	70 µL DMSO
DMSO	C	n.a.
EdU reaction buffer	D	36 mL DI H_2O
EdU buffer additive (10 x)	F	2 mL DI H_2O
Hoechst 33342	G	n.a.

Table 10. Composition of Click-iT® kit cocktails for 10 chambers

Component	Dilution	Required amount
1X Click-iT® EdU reaction buffer	180 µL + 1620 µL	1800 µL
CuSo4	80 µL	80 µL
Alexa Fluor® azide	5 µL	5 µL
Click-iT® EdU buffer additive	20 µL + 180 µL	200 µL
Total amount	2085 µL	2ml

Protocol to use Click-iT® EDU Alexa Fluor 555 Imaging kit solution.

1. Remove the medium from the chambers.
2. Add 1 ml of 3.7 % Paraformaldehyde into the chambers and incubate them for 15 mins at room temperature.
3. Remove the fixative solution and wash the solution with 3% BSA dissolved in PBS two times.
4. Add of 1 ml of 0.5 % Triton X-100 in PBS into the chambers and incubate the chambers for 20 mins.

5. Prepare the cocktail from the stock solution for 10 chambers.
6. Remove the permeabilizing solution from the chambers and wash with 3% BSA dissolved in PBS two times.
7. Add the 200 µl of cocktails in each chambers and cover with coverslip.
8. Keep the chambers in a dark place.
9. Incubate the chambers for 45 mins at room temperature.
10. Remove the cocktail mixture and wash the chambers with 3% BSA dissolved in PBS, one time.
11. Remove the wash solution and wash the chambers with PBS one time.
12. Prepare Hoechst Dye 33342 by adding 1 ul of dye to 2 ml of PBS and mix it.
13. Add 200 µl of solution onto the chambers and cover it with coverslip.
14. Keep the chambers in a dark place.
15. Incubate the chambers for 45 mins at room temperature.
16. Remove the solution from chambers and wash the chambers with PBS one time.
17. Add the mounting media and let them dry overnight.
18. Chambers are ready for capturing the image through Brightfield BX-50 fluorescence microscopy system.

APPENDIX D

This appendix lists the extended identification of plasma membrane channels in human keratinocytes.

Table 11. Transcripts for Ca^{2+} influx pathways (extended)

Gene Stable ID	Gene description	Transcript (RPKM)
ENSG00000102452	Sodium leak channel, non-selective [Acc:HGNC:19082]	0.4
ENSG00000153956	Calcium voltage-gated channel auxiliary subunit alpha2delta 1 [Acc:HGNC:1399]	0.3
ENSG00000165995	Calcium voltage-gated channel auxiliary subunit beta 2 [Acc:HGNC:1402]	0.3
ENSG00000171631	Pyrimidinergic receptor P2Y6 [Acc:HGNC:8543]	0.3
ENSG00000110881	Acid sensing ion channel subunit 1 [Acc:HGNC:100]	0.3
ENSG00000142408	Calcium voltage-gated channel auxiliary subunit gamma 8 [Acc:HGNC:13628]	0.3
ENSG00000006283	Calcium voltage-gated channel subunit alpha1 G [Acc:HGNC:1394]	0.2
ENSG00000148408	Calcium voltage-gated channel subunit alpha1 B [Acc:HGNC:1389]	0.2
ENSG00000102001	Calcium voltage-gated channel subunit alpha1 F [Acc:HGNC:1393]	0.2
ENSG00000083454	Purinergic receptor P2X 5 [Acc:HGNC:8536]	0.2
ENSG00000119121	Transient receptor potential cation channel subfamily M member 6 [Acc:HGNC:17995]	0.2
ENSG00000175591	Purinergic receptor P2Y2 [Acc:HGNC:8541]	0.2
ENSG00000198216	Calcium voltage-gated channel subunit alpha1 E [Acc:HGNC:1392]	0.2
ENSG00000067191	Calcium voltage-gated channel auxiliary subunit beta 1 [Acc:HGNC:1401]	0.2
ENSG00000213199	Acid sensing ion channel subunit 3 [Acc:HGNC:101]	0.2
ENSG00000144481	Transient receptor potential cation channel subfamily M member 8 [Acc:HGNC:17961]	0.2
ENSG00000162572	Sodium channel epithelial 1 delta subunit [Acc:HGNC:10601]	0.2

ENSG00000137672	Transient receptor potential cation channel subfamily C member 6 [Acc:HGNC:12338]	0.2
ENSG00000182389	Calcium voltage-gated channel auxiliary subunit beta 4 [Acc:HGNC:1404]	0.1
ENSG00000166862	Calcium voltage-gated channel auxiliary subunit gamma 2 [Acc:HGNC:1406]	0.1